Numerical Simulation of Boundary-Layer Excitation by Surface Heating/Cooling

Alvin Bayliss*
Exxon Corporate Research Science Laboratories, Annandale, New Jersey
Lucio Maestrello†
NASA Langley Research Center, Hampton, Virginia
Paresh Parikh‡
Vigyan Research Associates Inc., Hampton, Virginia
and
Eli Turkel§
Institute for Computer Applications in Science and Engineering, Hampton, Virginia

A numerical study of the concept of active control of growing disturbances in an unstable compressible flow by time-periodic, localized surface heating is presented. The simulations are calculated by a fourth-order-accurate solution of the compressible, laminar Navier-Stokes equations. Fourth-order accuracy is particularly important for this problem because the solution must be computed over many wavelengths. The numerical results demonstrate the growth of an initially small fluctuation into the nonlinear regime where a local breakdown into smaller scale disturbances can be observed. It is shown that periodic surface heating over a small strip can reduce the growth of the fluctuation provided that the phase of the heating current is properly chosen.

I. Introduction

TRANSITION in a boundary layer arises from the spatial growth and nonlinear saturation of unstable waves. A method of controlling or delaying transition is to introduce localized surface disturbances which can interfere with and reduce the level of the propagating disturbances. This concept was introduced by Liepmann et al.[1,2] They demonstrated that the introduction, in water, of localized, periodic temperature disturbances of appropriate phase could either enhance or reduce the overall level of fluctuations for a significant distance downstream. In addition, by measuring the fluctuating disturbance in the boundary layer upstream of the controlling surface, they were able to synthesize a signal to drive the cancellation disturbance at the controlling surface. This provided for active feedback control. An analysis by Maestrello and Ting[3] provided a theoretical justification for this method. The use of localized heating strips provides a control mechanism with a significantly lower expenditure of energy than that for passive control; for example, a steady heating of the entire surface.

Nosenchuk et al.[4] have demonstrated that localized surface heating can be used to trip the boundary layer and accelerate transition in air. Maestrello[5] has shown that localized surface heating in air can be used to trigger instantaneous transition. In addition, he showed that, by using feedback control to drive an acoustic disturbance, a significant reduction in the disturbance levels could be obtained. Thomas[6] demonstrated that a vibrating ribbon could be used to generate an unstable wave. In addition, he showed that by using a second ribbon downstream to generate an out-of-phase disturbance, the disturbance level could be reduced.

At the present time, the authors are not aware of any experiments that have shown a reduction in the level of a growing disturbance, *in air*, by using only localized surface heating. The use of localized heating to introduce an out-of-phase disturbance is considerably more delicate in air than in water. There are several reasons for this. First, much larger temperature disturbances are required to change the viscosity by an equivalent amount in air than in water.[5] In addition, in air $d\mu/dT>0$, which is destabilizing, while in water, $d\mu/dT<0$. Finally, in a compressible flow a temperature disturbance affects the pressure gradients via the equation of state in a manner that is difficult to analyze.

Localized surface heating has obvious attractions as a mechanism for active flow control for reasons of simplicity and efficiency. The primary objective of this paper is to demonstrate, using numerical solutions of the compressible Navier-Stokes equations, that time-periodic localized surface heating can be an effective technique to reduce the level of growing disturbances in air at flow velocities for which compressibility effects can be expected to be noticeable.

Our results demonstrate that localized temperature disturbances can be an effective technique to reduce the level of growing disturbances in the boundary layer. A localized disturbance over a one-quarter-wavelength-wide strip can reduce the level of the fluctuations. Other techniques, such as localized vibration, e.g., a vibrating ribbon, also offer potential. The greatest deficiency in the present program is the restriction to two-dimensional disturbances. In two dimensions, the development of instabilities and the transition to nonlinear behavior is very different than in three dimensions. The authors are currently developing a three-dimensional version of the code and will report the results from that study at a later time.

The simulations are based on solving the two-dimensional, compressible, Navier-Stokes equations using a fourth-order-accurate (in space) finite-difference scheme. It is our experience that a higher order accurate scheme is necessary to

Presented as Paper 85-0565 at the AIAA Shear Flow Control Conference, Boulder, CO, March 12-14, 1985; received April 23, 1985; revision received Sept. 10, 1985.

*Senior Staff Scientist. Member AIAA.
†Aerospace Technologist. Associate Fellow AIAA.
‡Research Engineer. Member AIAA.
§Visiting Scientist; currently, Professor, Tel-Aviv University, Tel-Aviv, Israel.

compute the solutions appropriate to this problem. In Sec. II we describe the model. In Sec. III we discuss the numerical results, and in Sec. IV the conclusions are presented.

II. Computational Model

The full Navier-Stokes equations written in conservation form are considered:

$$W_t + F_x + G_y = 0 \tag{1}$$

Here W is the vector $(\rho, \rho U, \rho V, E)^T$, ρ the density, U and V the x and y components of velocity, and E the total internal energy. The forms of the flux functions F and G are standard and will not be reproduced here for brevity. All viscous terms are retained.

The computational domain is the rectangle shown in Fig. 1. A steady solution is computed given an inflow boundary-layer profile.[7] Unsteady solutions are generated by modifying the inflow data by adding a perturbation of the following form to the mean:

$$\epsilon \text{Real Part}\{F(y)e^{i\omega t}\} \tag{2}$$

Here ϵ is the amplitude of the disturbance, and ω a frequency for which there is a spatially unstable eigenfunction $F(y)$ for the inflow profile. The eigenfunction is obtained from the corresponding Orr-Sommerfeld equation for the inflow profile (assuming, for simplicity, incompressible flow). For an inflow Mach number of 0.4 (which is used in all of the calculations herein), we have found that during the initial stage of growth the behavior of the solution is well predicted by neglecting compressibility. Compressibility becomes more important as the disturbance grows and temperature and density fluctuations become large. The code is written in conservation form and, therefore, can handle any Mach number, including transonic problems with shock development.

The resolution requirements for this problem are severe. The disturbance must be followed over a relatively large number of wavelengths, and it is necessary to prevent an accumulation of phase errors. Thus, the problem shares the difficulties of both fluid dynamics and wave propagation. In addition, smaller scale structures, requiring still more resolution, will be generated by nonlinear interactions. It is our experience that approximately ten points per wavelength (in the x direction) are necessary to give acceptable results. In addition, more resolution in the boundary layer is required than for steady flows. This density of grid points is necessary to resolve the wave propagation and the Orr-Sommerfeld eigenfunction normal to the plate. These requirements are greatly reduced by using the fourth-order scheme. The advantages of higher order methods for the numerical computation of waves have been well documented,[8,9] and it is well known that numerical errors in approximating the convective terms of Eq. (1) can cause a numerical dissipation which reduces the effective Reynolds number in viscous regions. For this reason, we use a scheme which is a simple modification of the second-order MacCormack scheme that is fourth-order accurate on the inviscid terms and second-order accurate on the viscous terms.[10]

For the one-dimensional equation,

$$W_t + F_x = 0$$

we have

$$\bar{W}_i^{n+1} = W_i^n - \frac{\Delta t}{6\Delta x}[7(F_{i+1}^n - F_i^n) - (F_{i+2}^n - F_{i+1}^n)] \tag{3a}$$

$$W_i^{n+1} = \frac{1}{2}\left[\bar{W}_i^{n+1} + W_i^n - \frac{\Delta t}{6\Delta x}\{7(\bar{F}_i^{n+1} - \bar{F}_{i-1}^{n+1}) - (\bar{F}_{i-1}^{n+1} - \bar{F}_{i-2}^{n+1})\}\right] \tag{3b}$$

The scheme [Eqs. (3)] becomes fourth order when alternated with a symmetric variant. It has a greatly reduced truncation error compared with the second-order MacCormack scheme. Our experience has been that fourth-order accuracy is necessary to efficiently compute the class of problems considered here. Operator splitting is used so that the two-dimensional system [Eq. (1)] is solved by successive applications of one-dimensional solution operators of the form of Eqs. (3). The computer program has been fully vectorized on the CDC VPS32 at NASA Langley Research Center and has been validated by comparing with known steady-state solutions and by comparing, in the linear regime, the growth rates obtained from imposing unstable disturbances on a mean flow with those predicted by linear theory.

In order to complete the description of the numerical scheme, it is necessary to describe the implementation of the boundary conditions. We distinguish between boundary conditions which must be imposed as part of the problem and those that are necessary because the straightforward application of the difference formula [Eqs. (3)] is not valid at the boundary points.

Consider the forward predictor, Eq. (3a). If $i=N$ denotes a boundary point, then the values of F_i are not available for $i>N$ and, thus, the scheme [Eq. (1)] cannot be applied at the points $i=N-1$ and N. The most satisfactory boundary treatment we have found is to define F_i for $i>N$ by third-order extrapolation from the interior (see Ref. 9). Hence, F_{N+1} and F_{N+2} are defined by

$$F_{N+1} = 4F_N - 6F_{N-1} + 4F_{N-2} - F_{N-3}$$

$$F_{N+2} = 4F_{N+1} - 6F_N + 4F_{N-1} - F_{N-2} \tag{4}$$

In Eq. (4) the extrapolated fluxes include both the viscous and inviscid terms.

In addition to the numerical boundary treatment described above, it is necessary to discuss those boundary conditions that must be imposed. At the plate, the two velocity components are set to zero and the temperature is specified. Several different techniques have been used to obtain the pressure. These include different orders of extrapolation in the normal direction and the use of the normal momentum equation. The accuracy of the solution is insensitive to the boundary treatment (probably because of the stretched grid). At present we simply use first-order extrapolation for the pressure.

The treatment of the upper boundary (see Fig. 1) is based on the linearized characteristics in the normal direction. The Navier-Stokes equations can be written in generic form, Eq. (1). In the normal direction we consider only the system,

$$U_t = G_y \tag{5}$$

In the applications, the vertical velocity v is small and positive at the upper boundary. Upon linearizing Eq. (5) we find that the three characteristic variables

$$p + \rho\tilde{c}^2, \qquad p + \tilde{\rho}\tilde{c}v, \qquad u \tag{6a}$$

are convected to the boundary from the interior. These three variables are obtained by zeroth-order extrapolation from the interior. Since we consider the linearized characteristics, the quantities with a tilde in Eq. (6a) are taken from the previous time step. The final boundary condition is obtained from setting

$$p_t - \tilde{\rho}\tilde{c}v_t = 0 \tag{6b}$$

corresponding to the characteristic variable entering the computational region. The use of the radiation condition, Eq. (6b), was previously found to considerably accelerate the convergence to the steady state and permit the upper boundary to be brought closer to the plate.[11]

A fluctuating disturbance is introduced at the inflow. Since this is a subsonic flow, three boundary conditions must be imposed at the inflow. These conditions are obtained by computing an eigenfunction of the Orr-Sommerfeld equations (using a program developed by R. Dagenhart of NASA Langley Research Center). The real part of the solution—times $e^{i\omega t}$—is then used to compute the three linearized characteristic variables which enter the computational domain from the outside. Specifically,

$$\left.\begin{matrix} p+\tilde{\rho}\tilde{c}u \\ p-\rho\tilde{c}^2 \end{matrix}\right\} = \text{mean} + \epsilon \begin{pmatrix} \text{values from} \\ \text{Orr-Sommerfeld equation} \end{pmatrix} \quad (7)$$

where ϵ determines the strength of the disturbance. The outgoing characteristic variable $p-\tilde{\rho}\tilde{c}u$ is obtained from the interior by zeroth-order extrapolation.

The outflow boundary condition is treated similarly. The incoming characteristic variable is set equal to zero by imposing the condition

$$p_t - \tilde{\rho}\tilde{c}u_t = 0 \quad (8)$$

The use of the condition [Eq. (8)] and more accurate radiation conditions to compute unsteady disturbances in subsonic flows is discussed in Ref. 11. Characteristic radiation boundary conditions of the form of Eq. (8) are commonly used in two-dimensional linear wave propagation problems (see, for example, Ref. 12). These boundary conditions have been found to be sufficiently accurate for the present calculations. This is based on comparisons with linear stability theory.

III. Results

In this section numerical results obtained from the code are described. This section will be divided into two parts. First, results for uncontrolled spatial disturbances evolving into a nonlinearly distorted fluctuation will be presented. In the second part, the effect of active control procedures will be demonstrated.

The basic model is described in Fig. 1. The mean flow is a boundary layer. The freestream Mach number is 0.4, and the unit Reynolds number is 3.0×10^5. The computational domain is chosen so that $Re_{\delta^*}=998$ at inflow and $Re_{\delta^*}=1730$ at outflow (where Re_{δ^*} is Reynolds number based on displacement thickness). This distance corresponds to approximately $200\delta_I$, where δ_I is the boundary-layer thickness at the inflow. A fluctuating disturbance is introduced at inflow with nondimensional frequency $F=(2\pi f\nu/U_\infty^2)$ of 0.8×10^{-4}. (Here f is the frequency, ν the kinematic viscosity, and U_∞ the freestream velocity.) This frequency is linearly unstable for Re_{δ^*} used at the inflow. A typical grid size for the calculations is 251×66 parallel and normal to the plate, respectively. We have used an exponential stretching in the normal direction. To obtain a more accurate solution for regions where nonlinear distortion is evident, a larger grid of 313×80 has also been used. The computational domain in the vertical direction extended over three boundary-layer thicknesses. In practice, the mean profile was computed with a considerably coarser grid and interpolated to the fine grid. The program was then run for a short time with the fine grid in order to smooth out any interpolation errors.

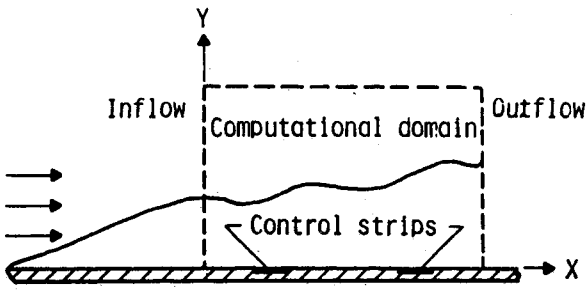

Fig. 1 Computational domain.

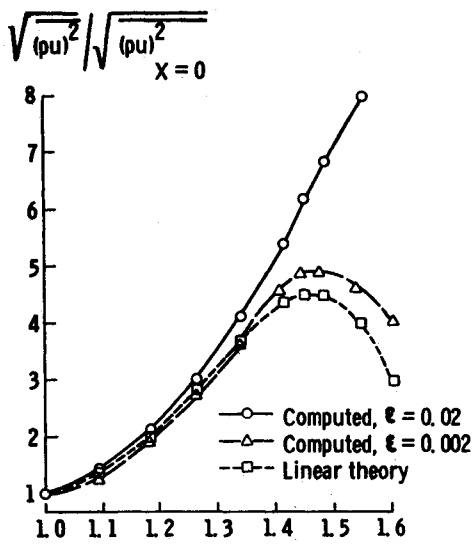

Fig. 2 Comparison of amplitude growth with linear theory.

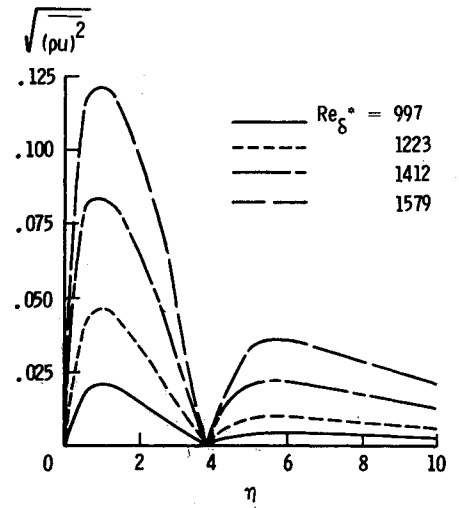

Fig. 3 Growth of rms amplitude vs η $(=(y/x)\sqrt{Re_x})$.

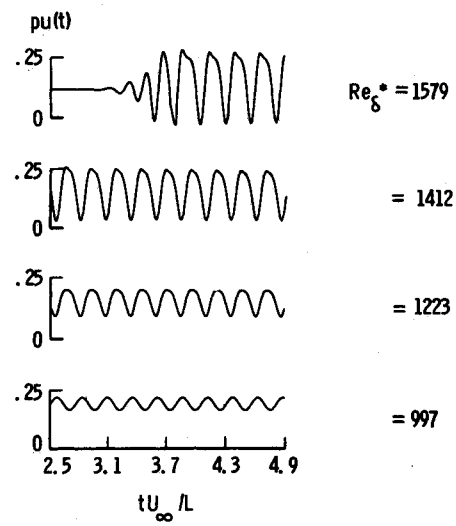

Fig. 4 Growth of $\rho u(t)$ vs time for $y=0.0115\delta_I$.

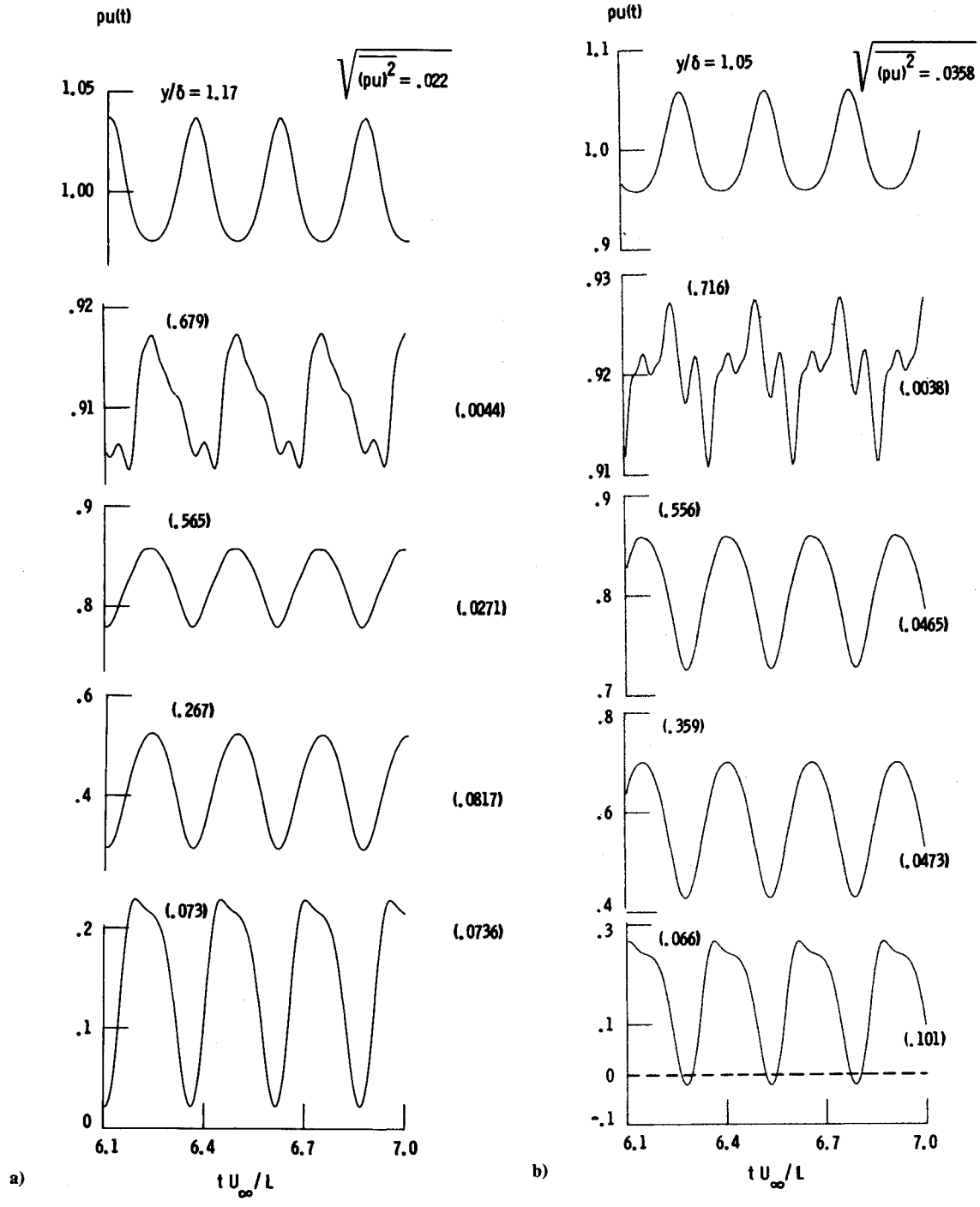

Fig. 5 Instantaneous $\rho u(t)$ across the boundary layer at a) $Re_{\delta^*} = 1412$, b) $Re_{\delta^*} - 1579$, $L = 1$.

Uncontrolled Results

In Fig. 2, spatial growth rates are shown for two different amplitudes of the inflow disturbance and compared with those obtained from linear incompressible theory.[13] The growth rates are obtained from computing the root-mean-square (rms)$(\sqrt{(\rho u - (\rho u)_{\text{mean}})^2})$ at different y locations and integrating the results with respect to y.

The results in Fig. 2 indicate good agreement with linear theory for a small initial disturbance (i.e., peak disturbance of 0.2% of freestream). In particular, the regions of growth and decay follow the linear theory predictions. For larger disturbances (i.e., 2% of freestream), nonlinear effects become important and the solution shows a definite departure from the linear theory.

Based on the wavelength of the disturbance at inflow, the computational domain extends over approximately 20 wavelengths during which the disturbance grows by a factor of approximately 10. The results of Fig. 2 were also validated by mesh refinement. A resolution of approximately 10 points per wavelength (at inflow; the wavelength gets smaller downstream) was required to give acceptable results. This is due to the fourth-order accuracy of the algorithm. In regions where nonlinear distortion was evident, more resolution was required to simulate the smaller scales. Approximately 30 points in the boundary layer (based on δ_I) were required to resolve the fluctuating disturbance. The second-order scheme with comparable grids consistently predicted either decay or greatly reduced growth rates.

In Fig. 3, $(\sqrt{((\rho u) - (\rho u)_{\text{mean}})^2})$ is plotted as a function of $\eta = (y/x)\sqrt{Re_x}$ for several different downstream locations. These profiles are similar to those obtained by Murdock for incompressible flows.[14] It is apparent that the basic shape of

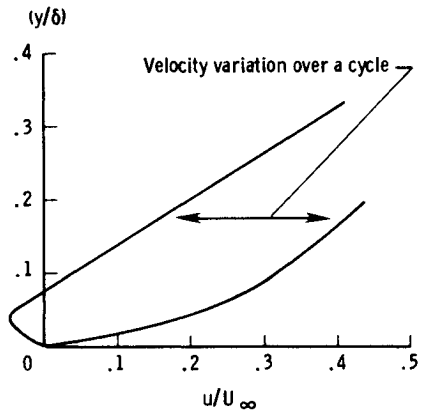

Fig. 6 Velocity profile at the extreme of a time cycle at $Re_{\delta^*} = 1547$.

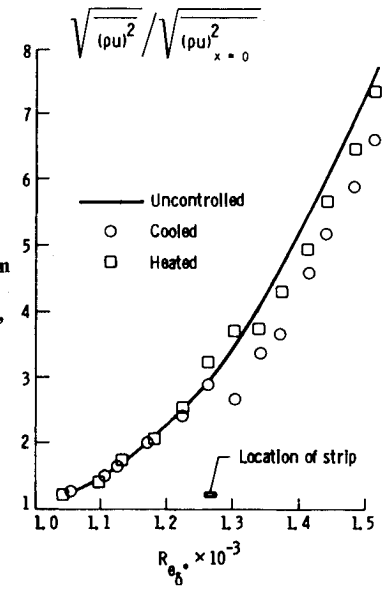

Fig. 7 Effect of control on rms amplitude growth with control strip at $Re_{\delta^*} = 1263$, $b/\delta^* = 3.98$.

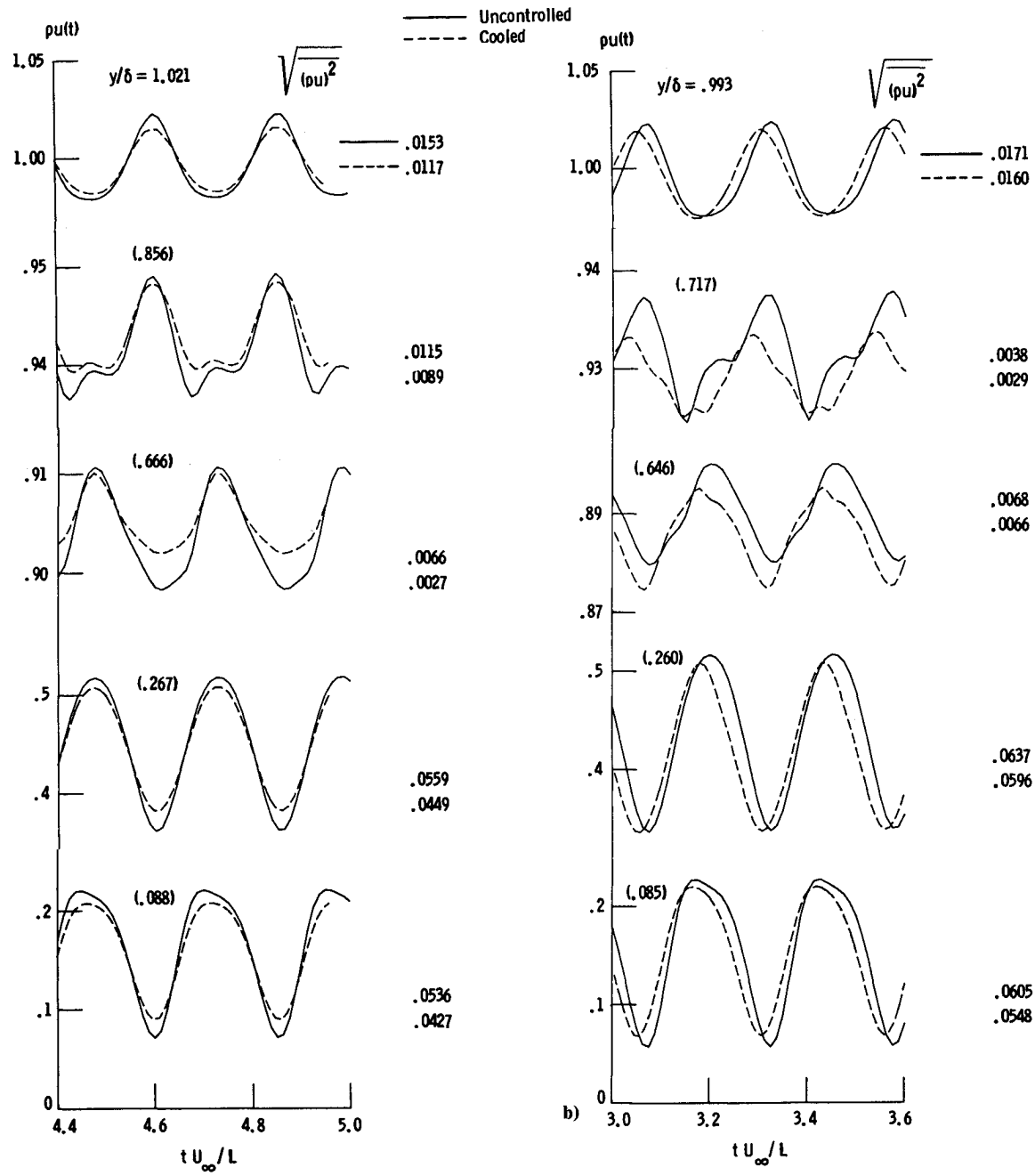

Fig. 8 Comparison of $\rho u(t)$ between controlled and uncontrolled cases: a) cooled at $Re_{\delta^*} = 1320$, b) heated at $Re_{\delta^*} = 1340$.

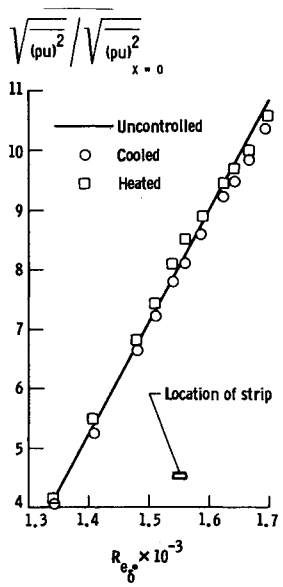

Fig. 9 Effect of control on rms amplitude growth with control strip at $Re_{\delta^*} = 1547$, $b/\delta^* = 1.6$.

the inflow profile (i.e., the Orr-Sommerfeld solution) is maintained as the disturbance grows. Most of the nonlinear distortion was observed near the wall and near the point where the disturbance changed sign. We believe that this is because the derivatives of disturbances (in y) are changing most rapidly at these locations.

To examine the evolution of the disturbance, $\rho u(t)$ is plotted in Fig. 4 as a function of (nondimensional) time for a fixed y location ($y = 0.0115\delta_I$). In Fig. 5 $\rho u(t)$ is plotted against t for several different y locations for $Re_{\delta^*} = 1412$ and 1579. It is apparent from these figures that a significant laminar growth has occurred between $Re_{\delta^*} = 1412$ and 1579. In addition, at the second station, $\rho u(t)$ at $y/\delta = 0.066$ becomes negative for part of the cycle indicating a cyclical separation and reattachment of flow on the plate. This phenomenon is further clarified in Fig. 6, where the instantaneous velocity profile is plotted at the two extrema of a time cycle close to the wall.

The disturbance, with an initial peak value of 2% of the freestream, has grown so large that the flow separates close to the wall and reattaches cyclically. By reducing the amplitude of inflow disturbances (but large enough to exhibit nonlinear effects) the laminar separation occurs further downstream. If three-dimensional effects are accounted for, the lateral spreading will limit the maximum growth of the disturbance, thus preventing the laminar separation.

Control Results

The effect of the active control was investigated at two stations with the control strip located at $Re_{\delta^*} = 1263$ and 1547. Surface heating and cooling were accomplished by modifying the temperature boundary condition over a small strip on the plate. The formula was

$$\frac{T}{T_{\text{ref}}} = \frac{T_w}{T_{\text{ref}}} \pm (\alpha + \beta \sin(\omega t + \phi))^2 \tag{9}$$

with the plus sign for heating and the minus sign for cooling. In Eq. (9), T_w is the temperature of the wall (520°R), and T_{ref} the reference temperature. The functional form of Eq. (9) models a dc (α) and an ac (β) current with phase ϕ.

In Fig. 7, the growth rates are compared with the uncontrolled case for a control strip located at $Re_{\delta^*} = 1263$. The width of the strip, b, is $b/\delta^* = 3.98$, where δ^* is the local displacement thickness. This corresponds to a width of approximately 20% of the disturbance wavelength at the inflow.

In Fig. 7, the parameters for the heated case were $\alpha = 1$, $\beta = 4$, and $\phi = 180$ deg, corresponding to a peak temperature of about 1650°R. For the cooled case the parameters were $\alpha = 1$, $\beta = 1.7$, and $\phi = 0$ deg, with a peak temperature of about 190°R. In the heating case, the temperature corresponds to roughly three times the unheated wall temperature, which is close to the temperature obtained in Ref. 5 using a tungsten wire. In the cooled case, the parameters are chosen so that the temperature will stay in the range where Sutherland's law is valid for the viscosity as a function of the temperature. Such a periodic cooling is not attainable by experimental techniques currently available. There were no numerical instabilities due to the large temperature perturbation, but the heating forced a reduction in the allowed time step.

The results in Fig. 7 demonstrate that, by an appropriate choice of phase, a reduction in the growth of the fluctuating disturbance can be obtained by surface heating. This is in contrast to the case of static heating which, as is well known, destabilizes airflows. The maximum reduction in the growth rate is approximately 6% for heating and 12% for cooling. A larger degree of reduction could be obtained by using multiple control strips with independent amplitude and phase adjustments. It should be noted that the results in Fig. 7 are extremely sensitive to phase. For a different choice of phase, both heating and cooling can increase the growth of the fluctuating disturbance.

In Fig. 8, $\rho u(t)$ is plotted as a function of nondimensional time tU_∞/L comparing heated and uncontrolled fluctuations (Fig. 8a) and the cooled and uncontrolled fluctuations (Fig. 8b). The graphs are shown at an x location slightly downstream of the heating strip where maximum reduction occurs and the rms values of the fluctuations are shown in each case. The figures show a reduction in amplitude in both cases with a slight phase change introduced by the heating. In both cases the control appears to have only a slight effect on the structure of the waveform. The numerical simulation establishes the feasibility of reducing the amplitude of the fluctuations by heating and cooling. This is not the best control that can be achieved. The degree of control that is possible depends on the parameters used for the control and on the number and location of the strips. We have not systematically tried the possibilities.

The effect of control at the second station ($Re_{\delta^*} = 1547$) is expected to be different from that of the first station because of the cyclical separation and reattachment of the flow (Fig. 6). This flow reversal causes the temperature to be partly convected upstream and, thus, effective phase control is lost. In the downstream direction, although control is achieved for both heating and cooling, it is significantly reduced. This occurs because effective phase control is lost for a portion of the time cycle in the layers close to the wall (Fig. 9).

IV. Conclusion

The concept of localized, periodic, surface heating to control growing disturbances in a subsonic flow has been simulated numerically. It is found that by appropriate adjustment of the phase of the controlling disturbances, the growth rate of the fluctuation can be reduced provided that the disturbances are periodic and not too large. A more pronounced effect can be obtained by cooling although this technique is practical at the present time for steady state and very low frequency.

This work shows the mechanism of the active control. Larger reductions in amplitude can be obtained by using multiple control strips with proper phase relationships. The results show that the increased growth causes separation with distance. This is due to the large inflow disturbance level. The control in this region is much less effective because of the loss of phase control near the wall.

The limitation in this model is the restriction to two-dimensional flow, since three-dimensional effects become important further downstream. This may prevent the kind of

separation and reattachment experienced at the second station observed herein.

Acknowledgments

Research for the fourth author was supported by the National Aeronautics and Space Administration under NASA Contracts NAS1-16394, NAS1-17070, and NAS1-17130 while he was in residence at the ICASE, NASA Langley Research Center, Hampton, VA. Partial support was provided for the first author under Contract NAS1-17070, and for the third author under NASA Contract NAS1-17252.

References

[1]Liepmann, H. W., Brown, G. L., and Nosenchuck, D. M., "Control of Laminar-Instability Waves Using a New Technique," *Journal of Fluid Mechancis*, Vol. 118, 1982, pp. 187-200.

[2]Liepmann, H. W. and Nosenchuck, D. M., "Active Control of Laminar-Turbulent Transition," *Journal of Fluid Mechanics*, Vol. 118, 1982, pp. 201-204.

[3]Maestrello, L. and Ting, L., "Analysis of Active Control by Surface Heating," *AIAA Journal*, Vol. 23, July 1985, pp. 1038-1045.

[4]Nosenchuck, D. M., Bettes, W. H., and Liepmann, H. W., "Active Transition Fixing," private communication, 1983.

[5]Maestrello, L., "Active Transition Fixing and Control of Boundary Layers in Air," AIAA Paper 85-0564, March 1985, to be published in *AIAA Journal*, 1986.

[6]Thomas, A.S.W., "The Control of Boundary Layer Transition Using a Wave-Superposition Principle," *Journal of Fluid Mechanics*, Vol. 137, 1983, pp. 233-250.

[7]Harris, J. E. and Blanchard, D. K., "Computer Program for Solving Laminar, Transitional or Turbulent Compressible Boundary-Layer Equations for Two-Dimensional and Axisymmetric Flow," NASA TM 83207, 1982.

[8]Kreiss, H. O. and Oliger, J., "Comparison of Accurate Methods for the Integration of Hyperbolic Systems," *Tellus*, Vol. 24, 1972, pp. 119-225.

[9]Turkel, E., "On the Practical Use of Higher Order Methods for Hyperbolic Systems," *Journal of Computational Physics*, Vol. 35, 1980, pp. 319-340.

[10]Gottlieb, D. and Turkel, E., "Dissipative Two-Four Methods for Time-Dependent Problems," *Mathematics of Computation*, Vol. 30, 1976, pp. 703-723.

[11]Bayliss, A. and Turkel, E., "Far Field Boundary Conditions for Compressible Flows," *Journal of Computational Physics*, Vol. 48, 1982, pp. 182-199.

[12]Cohen, M. F. et al., "A Comparison of Paraxial and Viscous Silent Boundary Methods in Finite Element Analysis," Joint ASME-ASCE Mechanics Conference, University of Colorado, Boulder, 1981, pp. 67-80.

[13]Dagenhart, R., private communication, NASA Langley Research Center, Hampton, VA, 1983.

[14]Murdock, J. W., "A Numerical Study of Nonlinear Effects on Boundary-Layer Stability," *AIAA Journal*, Vol. 15, Aug. 1977, pp. 1167-1173.